Published in final edited form as:
Clin Exp Metastasis. 2013 June ; 30(5): 555–568. doi:10.1007/s10585-012-9560-7.

FAK inhibition decreases cell invasion, migration and metastasis in MYCN amplified neuroblastoma

Michael L. Megison,
University of Alabama, Birmingham, AL, USA

Jerry E. Stewart,
University of Alabama, Birmingham, AL, USA

Hugh C. Nabers,
University of Alabama, Birmingham, AL, USA

Lauren A. Gillory, and
University of Alabama, Birmingham, AL, USA

Elizabeth A. Beierle
1600 7th Avenue South, Lowder Building, Room 300, University of Alabama, Birmingham, AL 35233, USA

Elizabeth A. Beierle: elizabeth.beierle@childrensal.org

Abstract

Neuroblastoma, the most common extracranial solid tumor of childhood, is responsible for over 15 % of pediatric cancer deaths. We have shown that neuroblastoma cell lines overexpress focal adhesion kinase (FAK), a non-receptor protein tyrosine kinase that controls a number of tumorigenic pathways. In this study, we hypothesized that inhibition of FAK would result in decreased cellular migration and invasion in neuroblastoma cell lines, and decrease metastasis in a murine model. We utilized non-isogenic and isogenic MYCN human neuroblastoma cell lines and parallel methods of FAK inhibition. Cell viability, migration, and invasion assays were employed to assess the effects of FAK inhibition in vitro. A nude mouse model was utilized to determine the effects of FAK inhibition on in vivo liver metastasis. FAK knockdown with siRNA resulted in decreased invasion and migration in neuroblastoma cell lines, and the effects of siRNA-induced FAK inhibition were more pronounced in *MYCN* amplified cell lines. In addition, abrogation of FAK with a small molecule inhibitors resulted in decreased cell survival, migration and invasion in neuroblastoma cell lines, again most pronounced in cell lines with *MYCN* amplification. Finally, small molecule FAK inhibition in a nude mouse model resulted in a significant decrease in metastatic tumor burden in SK-N-BE(2) injected animals. We believe that FAK plays an important role in maintaining and propagating the metastatic phenotype of neuroblastoma cells, and this driver role is exaggerated in cell lines that overexpress MYCN. FAK inhibition warrants further investigation as a potential therapeutic target in the treatment of aggressive neuroblastoma.

Correspondence to: Elizabeth A. Beierle, elizabeth.beierle@childrensal.org.

Conflict of interest: The authors have no conflict of interest.

Electronic supplementary material The online version of this article (doi:10.1007/s10585-012-9560-7) contains supplementary material, which is available to authorized users.

Keywords

SK-N-BE(2); SK-N-AS; WAC2; SH-EP; MYCN; FAK; FAK Y397; PF-573; 228; Neuroblastoma; NVP-TAE226

Introduction

Neuroblastoma is the most common extracranial solid tumor of childhood. This tumor of neural crest origin is responsible for over 15 % of pediatric cancer deaths [1]. Despite recent advances in chemotherapeutic and surgical care, this tumor continues to carry a dismal prognosis for children presenting with advanced or metastatic disease, with a survival of only 18–30 % [2]. The primary adverse prognostic factor for neuroblastoma is amplification of the *MYCN* oncogene [3, 4]. Amplification of *MYCN* has been associated with metastases and increased neuroblastoma proliferation and cell survival in neuroblastoma [5]. Additionally, knockdown of *MYCN* with siRNA results in cell death and apoptosis in some neuroblastoma cell lines [6, 7].

Focal adhesion kinase (FAK) is a non-receptor protein tyrosine kinase that localizes to focal adhesions, and controls a number of cell signaling pathways including proliferation, viability and survival [8–11]. The inhibition of FAK activation has been found to affect a number of cellular pathways. FAK antisense oligonucleotides, or a dominant-negative FAK protein (FAK-CD), has been shown to cause decreased growth in human breast cancer cells and melanoma cells [12–15]. Silencing FAK expression with small interfering RNAs resulted in decreased migration of lung cancer cells and glioblastoma cells [16, 17]. In addition, a number of small molecule inhibitors of FAK have been reported in the literature. One of these inhibitors, PF-573, 228 [18] was shown to inhibit invasion and migration of breast cancer cells [19]. Recently, other small molecule FAK inhibitors, 1, 2, 4, 5-benzenetetraamine tetrahydrochloride (Y15) and TAE226 have been reported to inhibit the in vivo growth of breast and pancreatic cancers[20, 21], and gliomas and ovarian tumors [22–24], respectively.

Previous studies from our laboratory have revealed that both the abundance of FAK mRNA and the expression of FAK protein were significantly increased in aggressive human neuroblastomas [25, 26]. Since FAK was overexpressed in higher stage, more aggressive neuroblastomas, we hypothesized that inhibition of FAK would result in a less metastatic phenotype in neuroblastoma cell lines with a decrease in cell migration and invasion. In the current study, we showed that abrogation of FAK with RNA interference-mediated silencing and small molecule inhibitors led to decreased cellular migration and invasion that was more marked in *MYCN* amplified cell lines. In addition, we demonstrated that inhibition of FAK resulted in decreased growth of neuroblastoma metastases in vivo. We believe that targeting FAK may be another therapeutic strategy to employ when designing novel interventions for aggressive neuroblastomas.

Materials and methods

Cells and cell culture

Human neuroblastoma cell lines SK-N-AS (CRL-2137, American Type Culture Collection, ATCC, Manassas, VA) and SK-N-BE(2) (CRL-2271, ATCC) were maintained in Dulbecco's modified Eagle's medium containing 10 % fetal bovine serum, 1 μg/mL penicillin and 1 μg/mL streptomycin and a 1:1 mixture of Eagle's Minimum Essential Medium and F12 with 10 % fetal bovine serum, 1 μg/mL penicillin and 1 μg/mL streptomycin, respectively.

The SH-EP (MYCN) and the isogenic WAC2 (MYCN +) cell lines were generously provided by Dr. M. Schwab (Deutsches Krebsforschungszentrum, Heidelberg, Germany). These cells have been described in detail previously [27]. Briefly, the parent cell line, SH-EP, is a *MYCN* non-amplified cell line. The SH-EP cell line was stably transfected with a vector containing *MYCN* to create the WAC2 MYCN overexpressing neuroblastoma cell line. These two cell lines were maintained in RPMI 1,640 medium supplemented with 10 % fetal bovine serum, 1 μg/mL penicillin and 1 μg/mL streptomycin.

Antibodies and reagents

Monoclonal anti-FAK (4.47) and rabbit polyclonal anti-phospho-FAK (Y397) antibodies were obtained from Millipore (05-537, EMD Millipore, Billerica, MA) and Invitrogen (4624G, Invitrogen Corp. Carlsbad, CA), respectively. Polyclonal antibody against MYCN was from cell signaling (9405, Cell Signaling Technology, Inc., Danvers, MA). Monoclonal antibodies against GAPDH (6C5) and β-actin were from Santa Cruz (Santa Cruz Biotechnology, Inc. Santa Cruz, CA). The small molecule PF-573-228 was obtained from Sigma-Aldrich Corp. (St. Louis, MO) and NVP-TAE226 was a generous gift of Novartis (Novartis Pharma AG, Basel Switzerland).

Western blotting

Cells or homogenized tumor samples were washed twice with cold 1× PBS and lysed on ice for 30 min in a buffer containing 50 mM Tris–HCL, (pH 7.5), 150 mM NaCl, 1 % Triton-X, 0.5 % NaDOC, 0.1 % SDS, 5 mM EDTA, 50 mM NaF, 1 mM $NaVO_3$, 10 % glycerol, and protease inhibitors: 10 μg/mL leupeptin, 10 μg/mL PMSF and 1 μg/mL aprotinin. The lysates were cleared by centrifugation at 10,000 rpm for 30 min at 4° C. Protein concentrations were determined using a Bio-Rad kit (BioRad, Inc., Hercules, CA). The boiled samples were loaded on Ready SDS–10 % PAGE gels (BioRad). Western blots were performed as previously described [26]. Briefly, antibodies were used according to manufacturer's recommended conditions. Molecular weight markers were utilized to confirm the expected size of the target proteins. Immunoblots were developed with chemiluminescence Renaissance Reagent (PerkinElmer Life Sciences, Inc., Waltham, MA). Blots were stripped with stripping solution (Bio-Rad) at 37° C for 15 min and then reprobed with selected antibodies. Immunoblotting with antibody to β-actin or GAPDH provided an internal control for equal protein loading.

siRNA transfection

Small interfering RNA's (siRNA) were obtained from Qiagen (Qiagen Inc. Valencia, CA) and used as previously described [26]. Briefly, cells were plated and allowed to attach for 24 h. The cells were transfected with Hyperfect (Qiagen) alone, Hyperfect (Qiagen) plus control siRNA (AllStars Negative Control siRNA, Qiagen), or Hyperfect (Qiagen) plus FAK siRNA [Hs_PTK2_10 FlexiTube siRNA (NM_005607, NM_153831), Qiagen] according to manufacturer's protocol. Cells were incubated for 24–72 h after transfection and then used for experiments.

Cell viability assays

Cells were treated with RNAi inhibition or PF-573, 228. Cell viability was measured using alamarBlue® assay. In brief, cells were plated 1.5×10^3 cells per well on 96-well culture plates and allowed to attach. Following treatment, 10 μL of alamarBlue® dye was added to 200 μL of cell medium. After 4–6 h, the absorbance at 595 nm was measured using a kinetic microplate reader (BioTek Gen5, BioTek Instruments, Winooski, VT).

Cellular invasion assay

Twelve-well culture plates with 8 micrometer micropore inserts were utilized for cell invasion assays. The top side of the insert was coated with Matrigel™ (BD Biosciences, San Jose, CA) (1 mg/mL, 50 μL for 4 h at 37° C). Cells were treated with RNAi inhibition or PF-573, 228 and 3×10^5 cells were placed into the upper well. The cells were cultured for 48 h and allowed to invade into the Matrigel™ layer. The cells on the inserts were fixed with 3 % paraformaldehyde, stained with crystal violet, and counted with a light microscope. Invasion was reported as fold change in number of cells invading into the Matrigel™.

Cellular migration assay

Twelve-well culture plates with 8 μm micropore inserts were utilized for cell migration assays. The bottom side of the insert was coated with collagen (10 mg/mL, 50 μL for 4 h at 37° C). Cells were treated with RNAi inhibition or PF-573, 228 and 5×10^3 cells were placed into the upper well. The cells were cultured for 24 h and allowed to migrate through the micropore insert. The cells on the inserts were then fixed with 3 % paraformaldehyde, stained with crystal violet, and counted with a light microscope. Migration was reported as fold change in number of cells migrating through the membrane.

Cellular migration was also measured utilizing a cell monolayer wounding (scratch) assay. Cells were plated onto 100 cm^2 culture plates and allowed to achieve 80 % confluence. The cells were then treated with RNAi and a standard scratch was placed on the plate utilizing a sterile, plastic 200 μL pipette tip. The plates were incubated for 48 h and photographs were obtained utilizing a Nikon Diaphot microscope system. The area of the scratch was quantified by measuring the pixel count of the scratched area and comparing it to the pixel count of the same plate at time zero.

Tumor growth in vivo

Female athymic nude mice, 6 weeks old, were purchased from Harlan Laboratories, Inc. (Chicago, IL). The mice were maintained in the SPF animal facility with standard 12 h light/dark cycles and allowed chow and water ad libitum. All experiments were performed after obtaining protocol approval by the animal care and use committee (100409104), and in compliance with the NIH animal use guidelines. A spleen injection model was utilized to induce hepatic metastasis. The animals were anesthetized with isoflurane and the spleen was exposed through a left flank incision. Human neuroblastoma cells, SK-N-AS (2×10^6) or SK-N-BE(2) (5×10^6), in 100 μL total volume were injected into the sub-capsular space of the spleen. After 24 h, under isoflurane anesthesia, the spleen was removed from the animals injected with the SK-N-AS cell lines. After two days, the animals began daily treatments with oral gavage of either control vehicle (methylcellulose, 100 μL, $N = 5$ per group) or TAE226 (60 mg/kg/day, in methylcellulose, 100 μL, $N = 5$ per group). This dose was chosen based upon reports in the literature demonstrating it to be the most well tolerated and also efficacious [24, 28, 29]. After 5 weeks of treatment, the animals were euthanized with CO_2 and bilateral thoracotomy, and the liver tissue was harvested and weighed. In addition, control murine liver weights were obtained from animals that did not undergo injection of tumor cells ($N = 5$).

Animal tissue samples and immunohistochemistry assays

A portion of the livers of the animals were snap frozen in liquid nitrogen for later use. The remaining portions of the livers were formalin-fixed and paraffin-embedded at the completion of the experiment. Blocks were cut with 8 micrometer sections for staining with hematoxylin and eosin or for immunohistochemistry for total and phosphorylated FAK as

previously described [25]. Briefly, for immunohistochemical staining, the slides were baked for 1 h at 70° C, deparaffinized, rehydrated, and steamed. The sections were then quenched with 3 % hydrogen peroxide and blocked with PBS-blocking buffer. The anti-FAK 4.47 mouse monoclonal antibody (05-537, EMD Millipore, 1:100) or rabbit polyclonal anti-phospho-FAK (Y397, 05-537, EMD Millipore, 1:200) antibodies were added and incubated overnight at 4° C. After washing with PBS, the secondary antibodies were added 1:250 dilution (Jackson Immuno Research Laboratories, Inc. West Grove, PA) for 1 h at 22° C. The staining reaction was developed with VECTASTAIN Elite ABC kit (PK-6100, Vector Laboratories, Burlingame, CA), TSA™ (biotin e reagent, 1:400, PerkinElmer, Inc. Waltham, MA) and DAB (Metal Enhanced DAB Substrate, Thermo Fisher Scientific, Rockford, IL). Slides were counterstained with hematoxylin. Negative controls (mouse IgG, 1 μg/mL, Invitrogen or rabbit IgG, 1 μg/mL, EMD Millipore) were included with each run.

Data analysis

Experiments were repeated at least in triplicate, and data reported as mean ± standard error of the mean. Densitometry of immunoblots was performed utilizing Scion Image Program (http://www.nist.gov/lispix/imlab/prelim/dnld.html). Bands were normalized to those of β-actin or GAPDH then compared to each other where appropriate. An ANOVA or Student's *t* test was used as appropriate to compare data between groups. Statistical significance was determined at the $p \leq 0.05$ level.

Results

FAK inhibition with RNA silencing led to decreased neuroblastoma invasion and migration

Previous data have shown that expression of focal adhesion kinase in human neuroblastoma cell lines was related to amplification of the *MYCN* oncogene, in that neuroblastoma cell lines with amplification of *MYCN* had an increased expression of FAK and were more dependent up on FAK for cell survival [25, 26]. Therefore, we chose two neuroblastoma cell lines with differing amplification status of the *MYCN* oncogene, the non-amplified SK-N-AS cell line [30] and the amplified SK-N-BE(2) cell line [31] for the current investigations (Supplemental Data Fig. 1a, b). SK-N-AS and SK-N-BE(2) neuroblastoma cell lines were treated with FAK siRNA for 48 h with the goal to achieve 20–30 % knockdown of the protein (Fig. 1a). This degree of FAK inhibition did not significantly affect cell survival as measured by alamarBlue® assay (Fig. 1b). However, when the cells were treated with FAK siRNA and cellular invasion was measured, the siRNA treatment of the *MYCN* amplified SK-N-BE(2) cells resulted in a decrease in invasion to 21 % compared to control untreated (100 %) or control siRNA (Fig. 1c). In the *MCYN* nonamplified SK-N-AS cell line treated with FAK siRNA, the number of invading cells decreased to 87 %, but this was not statistically significant from control untreated cells, or cells treated with control siRNA (Fig. 1c). Next, cell migration was examined. When the SK-N-BE(2) cells were treated with FAK siRNA, there was a significant decrease in cell migration, with only 46 % of the cells migrating through the membrane compared to control untreated cells (Fig. 1d). In the SK-N-AS cell line, again, the amount of migration was decreased (82 % compared to control untreated cells) but was not statistically significant (Fig. 1d). These results were confirmed with a cell monolayer wounding assay. Treatment with siRNA to FAK resulted in fewer cells migrating across the wounded monolayer that in the untreated group (Fig. 1e), with the most notable effects seen in the *MYCN* amplified SK-N-BE(2) cell line. These data were also shown in graphic form (Fig. 1f). Treatment with control siRNA did not affect invasion or migration in either cell line (Fig. 1c–f). These data demonstrated that FAK inhibition resulted in decreased cell migration and invasion that appeared to be more marked in the *MYCN* amplified SK-N-BE(2) cell line.

FAK inhibition with RNA silencing led to decreased neuroblastoma invasion and migration in a MYCN isogenic cell line

In the previous experiments, there was a difference in the effects of FAK inhibition up on cellular invasion and migration in the neuroblastoma cell lines based up on whether *MCYN* oncogene was amplified [SK-N-BE(2)] or not (SK-N-AS). Previous studies have shown that *MYCN* non-amplified neuroblastoma cell lines were less affected by FAK inhibition when cell survival was studied [21, 25]. In order to evaluate the effects of MYCN up on the findings with FAK inhibition in cellular invasion and migration, we next chose to utilize FAK siRNA in the isogenic MYCN ± neuroblastoma cell lines, WAC2 and SH-EP. These cell lines have been thoroughly described in previous publications [21, 27]. The parent cell line, SH-EP, is *MYCN* non-amplified. A stable cell line was created with a *MYCN* expression vector, and designated WAC2 (Supplemental Data Fig. 1c). Like the SK-N-BE(2) cell line, the MYCN + WAC2 cell line has greater FAK protein expression than the MYCN- SH-EP cell line (Supplemental Data Fig. 1d). The WAC2 and SH-EP isogenic neuroblastoma cell lines were treated with FAK siRNA for 24 h. Significant FAK knockdown was achieved in both cell lines (Fig. 2a). As noted with the SK-N-AS and SK-N-BE(2) cells, the degree of siFAK inhibition (40 nM for 24 h) did not result in decreased cell survival in either the SH-EP or WAC2 cell lines (Fig. 2b). When these cell lines were treated with FAK siRNA (40 nM), there was a decrease in cell invasion in the WAC2 cell line (Fig. 2c). The SH-EP cell line did not show a difference in invasion after FAK siRNA treatment (Fig. 2c). Next, cellular migration was assessed. SH-EP and WAC2 cells were treated with FAK siRNA (40 nM) and migration was evaluated after 24 h. There was a significant decrease in cell migration seen with the MYCN + WAC2 cells, but again, no significant decrease in the migration of the MYCN- SH-EP cells (Fig. 2d). These results were similar to those noted with the non-isogenic *MYCN* cell lines treated with siRNA. Treatment of the SH-EP and WAC2 cell lines with control siRNA did not affect invasion (Fig. 2c) or migration (Fig. 2d). These data further substantiated the findings that FAK inhibition had a greater effect up on invasion and migration in MYCN + than in MYCN– cell lines.

FAK inhibition with PF-573, 228 resulted in decreased neuroblastoma survival, invasion and migration

To provide collaborating evidence of our findings with siRNA, we chose to use the FAK kinase inhibitor, PF-573, 228. This molecule has been shown to interact with FAK and block its catalytic activity [18]. SK-N-AS and SK-N-BE(2) cell lines were treated with PF-573, 228 for 24 h at increasing concentrations. Immunoblotting demonstrated a negligible change in FAK phosphorylation in the SK-N-AS cell line, with a small decrease in total FAK seen only at high concentrations of PF-573, 228 (Fig. 3a, *blot and left graphs*). There was a marked decrease in FAK phosphorylation with little change in total FAK in the SK-N-BE(2) cell line (Fig. 3a, *blot and right graphs*), and this change in phosphorylation was seen at low concentrations of PF-573, 228 (Fig. 3a, *bottom right panel*). Cellular viability was measured using alamarBlue® assay following treatment with PF-573, 228 at increasing concentrations for 24 h. There was a significant decrease in cell viability in both cell lines, but significant effects were again noted at a lower concentration of PF-573, 228 in the *MCYN* amplified SK-N-BE(2) cell line (Fig. 3b). These two neuroblastoma cell lines were also treated with PF-573, 228 and invasion and migration were evaluated. FAK inhibition with PF-573, 228 resulted in decreased cell invasion and migration that was significant at a lower concentration of the PF-573, 228 in the *MYCN* amplified SK-N-BE(2) cell line compared to the *MYCN* non-amplified *SK*-N-AS cells (Fig. 3c, d). These changes were also apparent at concentrations of PF-573, 228 that were less than those affecting cellular survival. In addition, PF-573, 228 treatment of isogenic MYCN±cell lines (WAC2 and SH-EP) had similar effects, with the MYCN+WAC2 cells having a more profound response to FAK

inhibition than the MYCN-SH-EP cell line (Supplemental Data Fig. 2). The observed changes in the phenotype of the SK-N-AS cell line, since they occurred at concentrations of PF-573, 228 that showed little change in FAK phosphorylation, may have been due to off-target effects of the small molecule. However, the changes noted in the *MYCN* amplified SK-N-BE(2) cells were noted at concentrations of PF-573, 228 that were not only associated with a decrease in FAK phosphorylation (Fig. 3a), but were also well below the concentrations that affected cell survival (Fig. 3b). These PF-573, 228 data clearly showed that FAK abrogation resulted in a less metastatic phenotype that was more marked in the neuroblastoma cell line with *MYCN* amplification, following in the same vein as the findings seen with siRNA inhibition of FAK.

FAK inhibition resulted in decreased hepatic metastasis in a neuroblastoma nude mouse model

Because FAK inhibition decreased the invasion and migration and therefore, metastatic potential, of neuroblastoma cells in vitro, we hypothesized that inhibition of FAK would decrease the ability of neuroblastoma cells to form metastasis in vivo, and employed a nude mouse model to test this hypothesis. Neuroblastoma liver metastases were induced by injecting either SK-N-AS or SK-N-BE(2) tumor cells under the capsule of the spleen. The mice were treated with oral gavage of TAE226 or vehicle (methylcellulose). Since PF-573, 228 is not formulated for use in animals, TAE226 was chosen, as it is one of only a few small molecule FAK inhibitors that may be utilized in vivo. TAE226 treatment of SK-N-AS and SK-N-BE(2) cell lines resulted in decreased FAK phosphorylation (Supplemental Data Fig. 3), and also significantly decreased invasion and migration in the *MYCN* amplified SK-N-BE(2) neuroblastoma cell line (Supplemental Data Fig. 4, 5, respectively). After 5 weeks, the animals were euthanized and the livers were harvested and weighed. It was not possible to accurately count individual metastatic deposits in this model, so liver weight served as the measure of tumor burden. This method has been utilized by a number of investigators [32, 33] and is a well accepted method of measuring tumor burden within the liver. The weights of livers from non-injected control mice were included as a comparison (labeled “Control”). Liver metastasis formed in the mice injected with both *MYCN* non-amplified SK-N-AS (1.78 ± 0.51 vs. 0.56 ± 0.035 gm, $p = 0.002$, control vs. vehicle) and *MYCN* amplified SK-N-BE(2) (4.67 ±1.4 vs. 0.55 ± 0.042 gm, $p = 0.0006$, control vs. vehicle) tumor cells. However, the SK-N-BE(2) mice developed a significantly greater hepatic tumor load (1.78 ± 0.5 vs. 4.67 ± 0.51 gm, $p = 0.0004$, SK-N-AS vs. SK-N-BE(2)). Although the TAE226 treatment did not significantly change the weight of the animals, we know that the weight of the animal will influence the liver weight, so we also compared the tumor weight:animal weight ratios and found the results to remain unchanged; a significant difference was seen in the TAE226 treated SK-N-BE(2) and no significant difference in the mice with SK-N-AS tumors treated with TAE226 (data not shown).

The pattern of metastasis was also different for the two cell lines. Representative H & E staining of the livers from the animals at 20× is shown in Fig. 4b. The *MYCN* non-amplified SK-N-AS cells tended to form multiple deposits of tumor cells in the liver (Fig. 4b, *panel A, white arrow)* while the *MYCN* amplified SK-N-BE(2) cells metastasized in an infiltrative pattern (Fig. 4b, *panel C*). In the SK-N-AS injected mice treated with TAE226, there was no significant decrease in tumor burden compared to vehicle treated controls (1.78 ± 0.5 vs. 1.47 ± 0.37, vehicle vs. TAE226, p = NS) (Fig. 4a). However, in the SK-N-BE(2) injected mice, TAE226 significantly decreased the hepatic tumor burden compared to treatment with vehicle alone (4.67 ± 0.51 vs. 1.46 ± 0.29, vehicle vs. TAE226, $p < 0.001$) (Fig. 4a). These results were also evident on histopathology. There was little change in the liver and tumor histology in the *MYCN* non-amplified SK-N-AS animals treated with TAE226, with tumor deposits present within the liver (Fig. 4b, *panel B, white arrow*). After TAE226 treatment of

the *MYCN* amplified SK-N-BE(2) tumors, the pattern changed from the sheets of tumor cells infiltrating the liver seen in the vehicle treated animals (Fig. 4b, *panel C*), to only a few small deposits of tumor cells (Fig. 4b, *panel D, white oval)* scattered amongst normal appearing hepatocytes with normal hepatic architecture (Fig. 4b, *panel D, white box*). Tumor specimens were homogenized and the proteins evaluated by immunoblotting. SK-N-BE(2) tumors in animals treated with TAE226 had decreased phosphorylation of FAK and less FAK protein expression (Fig. 4c, *top panel*). When the SK-N-BE(2) tumor specimens were stained with immunohistochemistry (IHC) for total and phosphorylated FAK, it was also noted that hepatic metastasis from the animals treated with TAE226 had significantly less staining for FAK and less FAK Y397 phosphorylation (Fig. 4c, *right lower panels*) than those treated with vehicle alone (Fig. 4c, *left lower panels*). Representative photomicrographs of tumor specimens were presented in Fig. 4c. These data showed that FAK inhibition resulted in decreased metastatic potential of neuroblastoma cells in an in vivo hepatic metastasis model.

Discussion

In this study, we demonstrated that inhibition of focal adhesion kinase (FAK) with small interfering RNA and the small molecule PF-573, 228 resulted in decreased cell migration and invasion in neuroblastoma cell lines that was more marked in *MYCN* amplified cell lines. Further, these findings were seen in both isogenic and non-isogenic MYCN neuroblastoma cell lines. We also showed that inhibition of FAK slowed hepatic tumor metastatic growth in vivo. All of these factors are important elements in the maintenance of the metastatic phenotype of neuroblastoma cells.

Neuroblastoma tumors with amplification of the *MYCN* oncogene carry a worse prognosis due to increased metastatic potential [34]. Our previous studies showed that FAK expression in neuroblastoma cell lines and tumor specimens was correlated with amplification of the *MYCN* oncogene [25, 26]. Through dual luciferase assays, site-directed mutagenesis, and ChIP assays, it was demonstrated that MYCN bound to the FAK promoter and activated FAK expression in *MYCN* amplified neuroblastoma cell lines [26]. Further, we demonstrated with a number of different methods of FAK inhibition, that FAK abrogation in cell lines with MYCN overexpression, and more FAK expression, resulted in more marked increases in apoptosis and decreases in cell survival when compared with cells without *MYCN* amplification [21]. In the current study, we have seen these same trends with respect to invasion and migration. We utilized the non-isogenic SK-N-AS, non-amplified *MYCN*[30], and SK-N-BE(2), amplified *MYCN*[31], cell lines. Abrogation of FAK through multiple mechanisms including RNAi, resulted in decreased migration and invasion that was more marked in the cell line with *MYCN* amplification [SK-N-BE(2)]. Furthermore, the same results were noted in an isogenic MYCN±neuroblastoma cell line, one of the most important aspects of this study. These findings actually correlated well with those from other investigators studying kinase inhibition. We believe that these findings may be explained by the concept of oncogene addiction. Weinstein [35, 36] postulated that various tumor cells experience “oncogene addiction”, with certain cell lines being more physiologically dependent up on specific survival factors, and inhibition of these specific cellular factors has a more profound effect up on those cell lines than others of even the same tumor type.

Frisch and colleague [37] reported that the ability of cells to overcome anoikis, apoptosis resulting from the loss of cell–cell interactions, resulted in malignant transformation. They later demonstrated that FAK regulated anoikis [38], thereby playing a role in the malignant transformation of cells. In the current study we showed that the ability of neuroblastoma cells to migrate and invade was inhibited with abrogation of FAK. Since the focus of the current investigations was to evaluate the effect of FAK inhibition upon migration and

invasion, and cells that are not viable will not migrate or invade, we chose concentrations of siRNA that would inhibit FAK, but would not affect cellular survival. The siRNA-induced FAK inhibition did have a significant effect up on migration and invasion of the neuroblastoma cells, explaining the lack of detectable change in viability seen with the FAK siRNA treatment in these cell lines.

A small molecule FAK inhibitor, PF-573, 228, was also utilized in the current studies as a means to corroborate the siRNA findings. This compound has been shown to interact with FAK at the ATP binding pocket, blocking the catalytic activity of FAK [18]. In previous experiments, PF-573, 228 was shown to decrease adhesion and migration of human epithelial carcinoma cells [18] and small-cell lung cancer cells [39], and to enhance chemotherapy–induced cytotoxicity and apoptosis in multiple human pancreatic cell lines [40]. Wendt [19] proved that inhibiting FAK with PF-573, 228 decreased invasion and metastatic potential in human breast cancer cells through blocking the FAK activation of TGF β. To minimize off-target effects, PF-573, 228 was chosen for these investigations, over a very similarly related compound, PF-562, 271. PF562, 271 has also been utilized as a FAK inhibitor, but PF-562, 271 also has significant effects upon PyK2 [41] that PF-573, 228 does not have. In the current study, PF-573, 228 was effective in decreasing FAK phosphorylation in *MYCN* amplified neuroblastoma cell lines leading to significant changes in migration and invasion, but was not as effective in decreasing FAK phosphorylation in non-amplified cell lines. Unlike in the SK-N-BE(2) *MYCN* amplified cells, the PF-573, 228-induced phenotypic changes seen in the non-amplified SK-N-AS cell line were likely due to off-target effects of the molecule, a common finding when utilizing small molecules. However, these findings have extremely important therapeutic implications, in that they show that it may be more effective to target FAK in aggressive, *MYCN* amplified human tumors.

TAE226 (NVP-TAE226) have been previously described in the literature for its ability to inhibit FAK expression. TAE226 has been utilized in a number of studies as a FAK inhibitor. In human glioma [42] ovarian cancer [24] and a neuroblastoma [43] cell lines, treatment with TAE226 decreased FAK Y397 phosphorylation without affecting total FAK expression. In addition, this is one of only a few small molecule FAK inhibitors available for use for in vivo studies [28, 29]. These studies provided the background for utilizing TAE226 as a FAK inhibitor for the in vivo studies presented in the current manuscript.

In the current study we investigated the effects of FAK inhibition upon neuroblastoma hepatic metastasis. As seen with the in vitro data, the cell line with *MYCN* amplification and greater FAK expression, SK-N-BE(2), had a more significant decrease in hepatic tumor burden with FAK inhibition than the non-amplified *MYCN* and less FAK expressing SK-N-AS tumor cell line. There was also a notable change in the pattern of hepatic metastases in the SK-N-BE(2) tumors following FAK inhibition, with the diffuse infiltration of tumor cells changing to scattered tumor cell deposits. The ability to demonstrate in an animal model that FAK inhibition was relevant in metastatic neuroblastoma was an important aspect of the current study.

In conclusion, we believe that focal adhesion kinase plays an important role in the metastatic phenotype of neuroblastoma cells, and that this role is exaggerated in cell lines which overexpress MYCN and FAK. The increased dependence on FAK provides a target for therapy that may improve the survival of those select patients with *MYCN* amplified tumors, who presently carry the worst prognosis in this disease. We have shown that FAK inhibition warrants further investigation as a potential therapeutic target in the treatment of aggressive neuroblastoma.

Supplementary Material

Refer to Web version on PubMed Central for supplementary material.

Acknowledgments

The authors would like to thank Dr. Schwab for his kind gift of the SH-EP and WAC2 cell lines. The authors were supported in part by grants from the National Cancer Institute including MM, LG, (Grant Number T32CA091078) and EAB (Grant Number K08CA118178). The content of this manuscript was solely the responsibility of the authors and does not necessarily represent the official views of the National Cancer Institute or the National Institutes of Health.

References

1. Maris JM, Matthay KK. Molecular biology of neuroblastoma. J Clin Oncol. 1999; 17:2263–2279.
2. Cotterill SJ, Parker L, More L, Craft AW. Neuroblastoma: changing incidence and survival in young people aged 0–24 years. A report from the North of England young person's malignant disease registry. Med Pediatr Oncol. 2001; 36:231–234. [PubMed: 11464892]
3. Brodeur GM, Seeger RC, Schwab M, Varmus HE, Bishop JM. Amplification of N-myc in untreated human neuroblastomas correlates with advanced stage disease. Science. 1984; 224:1121–1124. [PubMed: 6719137]
4. Seeger RC, Brodeur GM, Sather H, Dalton A, Siegle SE, Wong KY, Hammond D. Association of multiple copies of the N-myc oncogene with rapid progression of neuroblastomas. N Engl J Med. 1985; 313:1111–1116. [PubMed: 4047115]
5. Zaizen Y, Taniguchi S, Noguchi S, Suita S. The effect of N-myc amplification and expression on invasiveness of neuroblastoma cells. J Pediatr Surg. 1993; 28:766–769. [PubMed: 8331499]
6. Kang JH, Rychahou PG, Ishola TA, Qiao J, Evers BM, Chung DH. MYCN silencing induces differentiation and apoptosis in human neuroblastoma cells. Biochem Biophys Res Commun. 2006; 351:192–197. [PubMed: 17055458]
7. Nara K, Kusafuka T, Yoneda A, Oue T, Sangkhathat S, Fukuzawa M. Silencing of MYCN by RNA interference induces growth inhibition, apoptotic activity and cell differentiation in a neuroblastoma cell line with MYCN amplification. Int J Oncol. 2007; 30:1189–1196. [PubMed: 17390021]
8. Schaller MD, Borgman CA, Cobb BS, Vines RR, Reynolds AB, Parsons JT. pp 125FAK a structurally distinctive protein-tyrosine kinase associated with focal adhesions. Proc Natl Acad Sci USA. 1992; 89:5192–5196. [PubMed: 1594631]
9. Hanks SK, Polte TR. Signaling through focal adhesion kinase. BioEssays. 1997; 19:137–145. [PubMed: 9046243]
10. Zachary I. Focal adhesion kinase. Int J Biochem Cell Biol. 1997; 29:929–934. [PubMed: 9375372]
11. Gabarra-Niecko V, Schaller MD, Dunty JM. FAK regulates biological processes important for the pathogenesis of cancer. Cancer Metastasis Rev. 2003; 22:359–374. [PubMed: 12884911]
12. Xu LH, Yang XH, Bradham CA, Brenner DA, Baldwin AS, Craven RJ, Cance WG. The focal adhesion kinase suppresses transformation-associated, anchorage-independent apoptosis in human breast cancer cells. Involvement of death receptor-related signaling pathways. J Biol Chem. 2000; 275:30597–30604. [PubMed: 10899173]
13. Xu LH, Yang XH, Craven RJ, Cance WG. The COOH-terminal domain of the focal adhesion kinase induces loss of adhesion and cell death in human tumor cells. Cell Growth Differ. 1998; 9:999–1005. [PubMed: 9869300]
14. Xu LH, Owens LV, Sturge GC, Yang X, Liu ET, Craven RJ, Cance WG. Attenuation of the expression of the focal adhesion kinase induces apoptosis in tumor cells. Cell Growth Differ. 1996; 7:413–418. [PubMed: 9052982]
15. Golubovskaya VM, Beviglia L, Xu LH, Earp HS, Craven RJ, Cance W. Dual inhibition of focal adhesion kinase and epidermal growth factor receptor pathways cooperatively induces death receptor-mediated apoptosis in human breast cancer cells. J Biol Chem. 2002; 277:38978–38987. [PubMed: 12167618]

16. Han EK, Mcgonigal T, Wang J, Giranda VL, Luo Y. Functional analysis of focal adhesion kinase (FAK) reduction by small inhibitory RNAs. Anticancer Res. 2004; 24:3899–3905. [PubMed: 15736429]

17. Lipinski CA, Tran NL, Menashi E, Rohl C, Kloss J, Bay RC, Berens ME, Loftus JC. The tyrosine kinase pyk2 promotes migration and invasion of glioma cells. Neoplasia. 2005; 7:435–445. [PubMed: 15967096]

18. Slack-Davis JK, Martin KH, Tilghman RW, Iwanicki M, Ung EJ, Autry C, Luzzio MJ, Cooper B, Kath JC, Roberts WG, Parsons JT. Cellular characterization of a novel focal adhesion kinase inhibitor. J Biol Chem. 2007; 282:14845–14852. [PubMed: 17395594]

19. Wendt MK, Schiemann WP. Therapeutic targeting of the focal adhesion complex prevents oncogenic TGF-beta signaling and metastasis. Breast Cancer Res. 2009; 11:R68. [PubMed: 19740433]

20. Golubovskaya VM, Nyberg C, Zheng M, Kweh F, Magis A, Ostrov D, Cance WG. A small molecule inhibitor, 1, 2, 4, 5-benzenetetraamine tetrahydrochloride, targeting the Y397 site of focal adhesion kinase decreases tumor growth. J Med Chem. 2008; 51:7405–7416. [PubMed: 18989950]

21. Beierle EA, Ma X, Stewart J, Nyberg C, Trujillo A, Cance WG, Golubovskaya VM. Inhibition of focal adhesion kinase decreases tumor growth in human neuroblastoma. Cell Cycle. 2010; 9:1005–1015. [PubMed: 20160475]

22. Golubovskaya VM, Virnig C, Cance WG. TAE226-induced apoptosis in breast cancer cells with overexpressed Src or EGFR. Mol Carcinog. 2008; 47:222–234. [PubMed: 17849451]

23. Liu TJ, LaFortune T, Honda T, Ohmori O, Hatakeyama S, Meyer T, Jackson D, deGroot J, Yung WK. Inhibition of both focal adhesion kinase and insulin-like growth factor-I receptor kinase suppresses glioma proliferation in vitro and in vivo. Mol Cancer Ther. 2007; 6:1357–1367. [PubMed: 17431114]

24. Halder J, Lin YG, Merritt WM, Spannuth WA, Nick AM, Honda T, Kamat AA, Han LY, Kim TJ, Lu C, Tari AM, Born-mann W, Fernandez A, Lopez-Berestein G, Sood AK. Therapeutic efficacy of a novel focal adhesion kinase inhibitor TAE226 in ovarian carcinoma. Cancer Res. 2007; 67:10976–10983. [PubMed: 18006843]

25. Beierle EA, Massoll NA, Hartwich J, Kurenova EV, Golubovskaya VM, Cance WG, McGrady P, London WB. Focal adhesion kinase expression in human neuroblastoma: immunohistochemical and real-time PCR analyses. Clin Cancer Res. 2008; 14:3299–3305. [PubMed: 18519756]

26. Beierle EA, Trujillo A, Nagaram A, Kurenova EV, Finch R, Ma X, Vella J, Cance WG, Golubovskaya VM. N-MYC regulates focal adhesion kinase expression in human neuroblastoma. J Biol Chem. 2007; 282:12503–12516. [PubMed: 17327229]

27. Schweigerer L, Breit S, Wenzel A, Tsunamoto K, Ludwig R, Schwab M. Augmented *MYCN* expression enhances the malignant phenotype of human neuroblastoma cells: evidence for induction of autocrine growth factor activity. Cancer Res. 1990; 50:411–416.

28. Hao HF, Takaoka M, Bao XH, Wang ZG, Tomono Y, Sakurama K, Ohara T, Fukazawa T, Yamatsuji T, Fujiwara T, Naomoto Y. Oral administration of FAK inhibitor TAE226 inhibits the progression of peritoneal dissemination of colorectal cancer. Biochem Biophys Research Commun. 2012; 423:744–749. [PubMed: 22705303]

29. Sakurama K, Noma K, Takaoka M, Tomono Y, Watanabe N, Hatakeyama S, Ohmori O, Hirota S, Motoki T, Shirakawa Y, Yamatsuji T, Haisa M, Matsuoka J, Tanaka N, Naomoto Y. Inhibition of focal adhesion kinase as a potential therapeutic strategy for imatinib-resistant gastrointestinal stromal tumor. Mol Cancer Ther. 2009; 8:127–134. [PubMed: 19139121]

30. Ucar K, Seeger RC, Challita PM, Watanabe CT, Yen TL, Morgan JP, Amado R, Chou E, McCallister T, Barber JR, Jolly DJ, Reynolds CP, Gangavalli R, Rosenblatt JD. Sustained cytokine production and immunophenotypic changes in human neuroblastoma cell lines transduced with a human gamma interferon vector. Cancer Gene Ther. 1995; 2:171–181. [PubMed: 8528960]

31. Nguyen T, Hocker JE, Thomas W, Smith SA, Norris MD, Haber M, Cheung B, Marshall GM. Combined RAR alpha- and RXR-specific ligands overcome N-myc-associated retinoid resistance in neuroblastoma cells. Biochem Biophys Res Comm. 2003; 302:462–468. [PubMed: 12615055]

32. Bandapalli OR, Paul E, Schirmacher P, Brand K. Opposite effects of tissue inhibitor of metalloproteinases-1 (TIMP-1) overexpression and knockdown on colorectal liver metastases. BMC Res Notes. 2012; 5:14. [PubMed: 22230683]
33. Hawcroft G, Volpato M, Marston G, Ingram N, Perry SL, Cockbain AJ, Race AD, Munarini A, Belluzzi A, Loadman PM, Coletta PL, Hull MA. The omega-3 polyunsaturated fatty acid eicosapentaenoic acid inhibits mouse MC-26 colorectal cancer cell liver metastasis via inhibition of prostaglandin E(2)-dependent cell motility. Br J Pharmacol. 2012; 166:1724–1737. [PubMed: 22300262]
34. Goodman LA, Liu BC, Thiele CJ, Schmidt ML, Cohn SL, Yamashiro JM, Pai DS, Ikegaki N, Wada RK. Modulation of N-myc expression alters the invasiveness of neuroblastoma. Clin Exp Metastasis. 1997; 15:130–139. [PubMed: 9062389]
35. Weinstein IB. Cancer. Addiction to oncogenes–the Achilles heal of cancer. Science. 2002; 297:63–64. [PubMed: 12098689]
36. Weinstein IB, Joe A. Oncogene addiction. Cancer Res. 2008; 68:3077–3080. [PubMed: 18451130]
37. Frisch SM, Francis H. Disruption of epithelial cell-matrix interactions induces apoptosis. J Cell Biol. 1994; 124:619–626. [PubMed: 8106557]
38. Frisch SM, Vuori K, Ruoslahti E, Chan-Hui PY. Control of adhesion-dependent cell survival by focal adhesion kinase. J Cell Biol. 1996; 134:793–799. [PubMed: 8707856]
39. Ocak S, Yamashita H, Udyavar AR, Miller AN, Gonzalez AL, Zou Y, Jiang A, Yi Y, Shyr Y, Estrada L, Quaranta V, Massion PP. DNA copy number aberrations in small-cell lung cancer reveal activation of the focal adhesion pathway. Oncogene. 2010; 29:6331–6342. [PubMed: 20802517]
40. Huanwen W, Zhiyong L, Xiaohua S, Xinyu R, Kai W, Tonghua L. Intrinsic chemoresistance to gemcitabine is associated with constitutive and laminin-induced phosphorylation of FAK in pancreatic cancer cell lines. Mol Cancer. 2009; 8:125. [PubMed: 20021699]
41. Roberts WG, Ung E, Whalen P, Cooper B, Hulford C, Autry C, Richter D, Emerson E, Lin J, Kath J, Coleman K, Yao L, Martinez-Alsina L, Lorenzen M, Berliner M, Luzzio M, Patel N, Schmitt E, LaGreca S, Jani J, Wessel M, Marr E, Griffor M, Vajdos F. Antitumor activity and pharmacology of a selective focal adhesion kinase inhibitor, PF-562, 271. Cancer Res. 2008; 68:1935–1944. [PubMed: 18339875]
42. Shi Q, Hjelmeland AB, Keir ST, Song L, Wickman S, Jackson D, Ohmori O, Bigner DD, Friedman HS, Rich JN. A novel low-molecular weight inhibitor of focal adhesion kinase, TAE226, inhibits glioma growth. Mol Carcinog. 2007; 46:488–496. [PubMed: 17219439]
43. Beierle EA, Trujillo A, Nagaram A, Golubovskaya VM, Cance WG, Kurenova EV. TAE226 inhibits human neuroblastoma cell survival. Cancer Invest. 2008; 26:145–151. [PubMed: 18259944]

Abbreviations

EDTA	Ethylenediaminetetraacetic acid
FAK	Focal adhesion kinase
NaDOC	Sodium deoxycholate
PMFS	Phenylmethanesulfonylfluoride

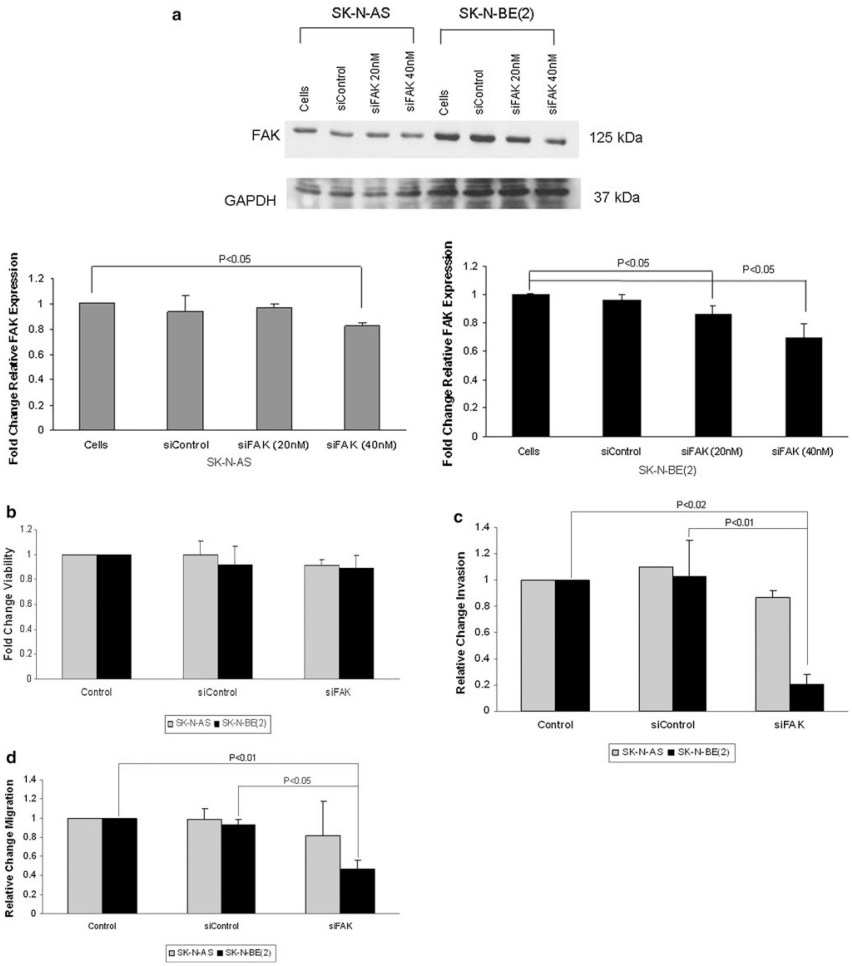

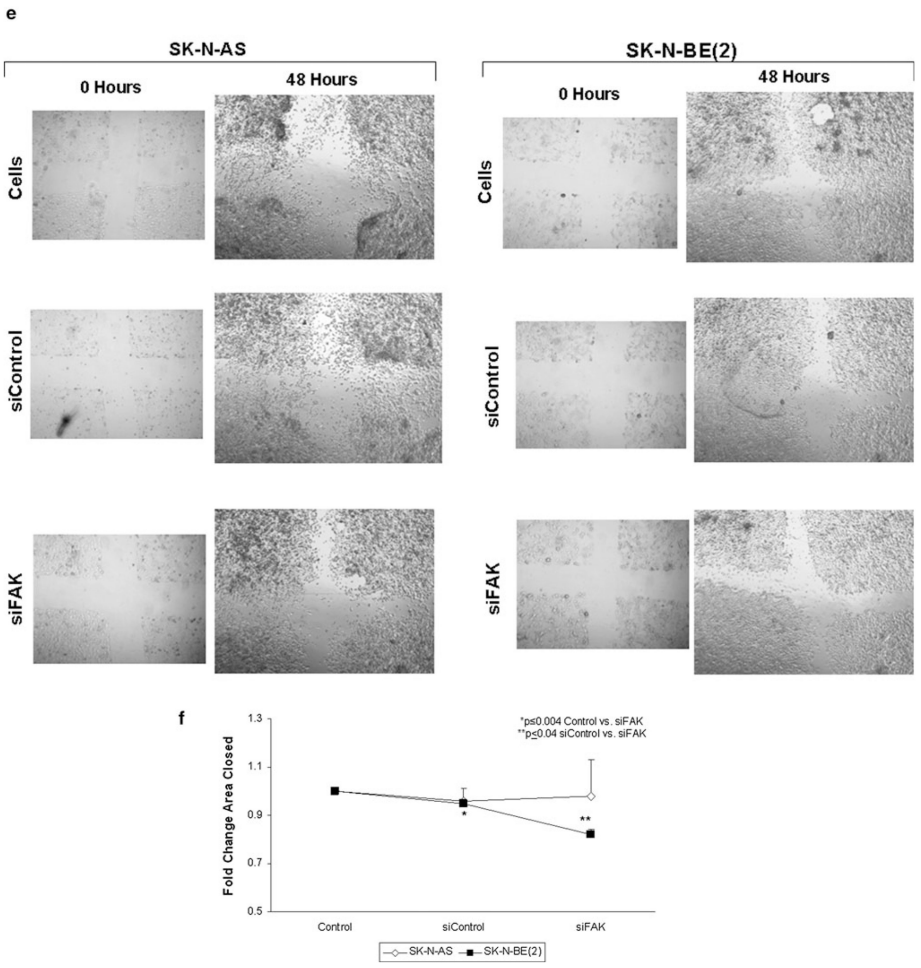

Fig. 1.

FAK inhibition with RNA silencing led to decreased neuroblastoma invasion and migration in *MYCN* amplified neuroblastoma cells. **a** SK-N-AS and SK-N-BE(2) neuroblastoma cell lines were treated with FAK siRNA or control siRNA. Immunoblotting was utilized to confirm FAK protein knockdown. After treatment with 40 nM FAK siRNA for 48 h, there was a significant decrease in FAK protein expression. Densitometry was utilized to quantitie FAK inhibition, expressed relative to the GAPDH bands (*bottom graphs*). **b** SK-N-AS and SK-N-BE(2) cell lines were treated with FAK siRNA at 40 nM for 48 h and cell viability was measured using alamarBlue® assays. There was no significant change in cellular viability in either cell line after siRNA treatment. The control siRNA had no effect on cellular viability. **c** SK-N-AS and SK-N-BE(2) cell lines were treated with FAK siRNA 40 nM for 48 h and allowed to invade through a Matrigel™ coated micropore insert. Invasion was reported as fold change. Cellular invasion was significantly decreased in the *MYCN* amplified SK-N-BE(2) cells with FAK inhibition. The *MYCN* non-amplified SK-N-AS cell line had a small decrease in invasion, but it did not reach statistical significance. Invasion was not affected by the control siRNA in either cell line. **d** SK-N-AS and SK-N-BE(2) cell lines were treated with FAK siRNA 40 nM for 48 h and allowed to migrate through a micropore insert. Migration was reported as fold change in number of cells migrating through the membrane. As with invasion, there was a significant decrease in cellular migration in the SK-N-BE(2) cells after FAK siRNA treatment, but no significant decrease in the SK-N-AS cell line. Also, migration was not affected by the control siRNA in either

cell line. **e** Migration was also measured with cell monolayer wounding assays. SK-N-AS and SK-N-BE(2) cells were allowed to achieve 80 % confluence and a standard scratch was placed. The cells were treated with FAK siRNA (40 nM) and the plates were incubated for 48 h. Photographs were obtained utilizing a Nikon Diaphot microscope system. In the SK-N-BE(2) cell line, siRNA-induced FAK inhibition resulted in a decrease in the amount of cells migrating into the scratched area (*right columns, bottom row*) compared to siControl or no treatment (*right columns, middle and top rows, respectively*). FAK siRNA did not significantly affect migration across the scratch in the SK-N-AS cell line (*left columns*). **f** The area of the scratch was quantified by measuring the pixel count of the scratched area and comparing it to the pixel count of the same plate at time zero. There was a significant decrease in the area of the scratch closed following FAK siRNA in the SK-N-BE(2) cell line. Migration was not affected in either cell line by the control siRNA

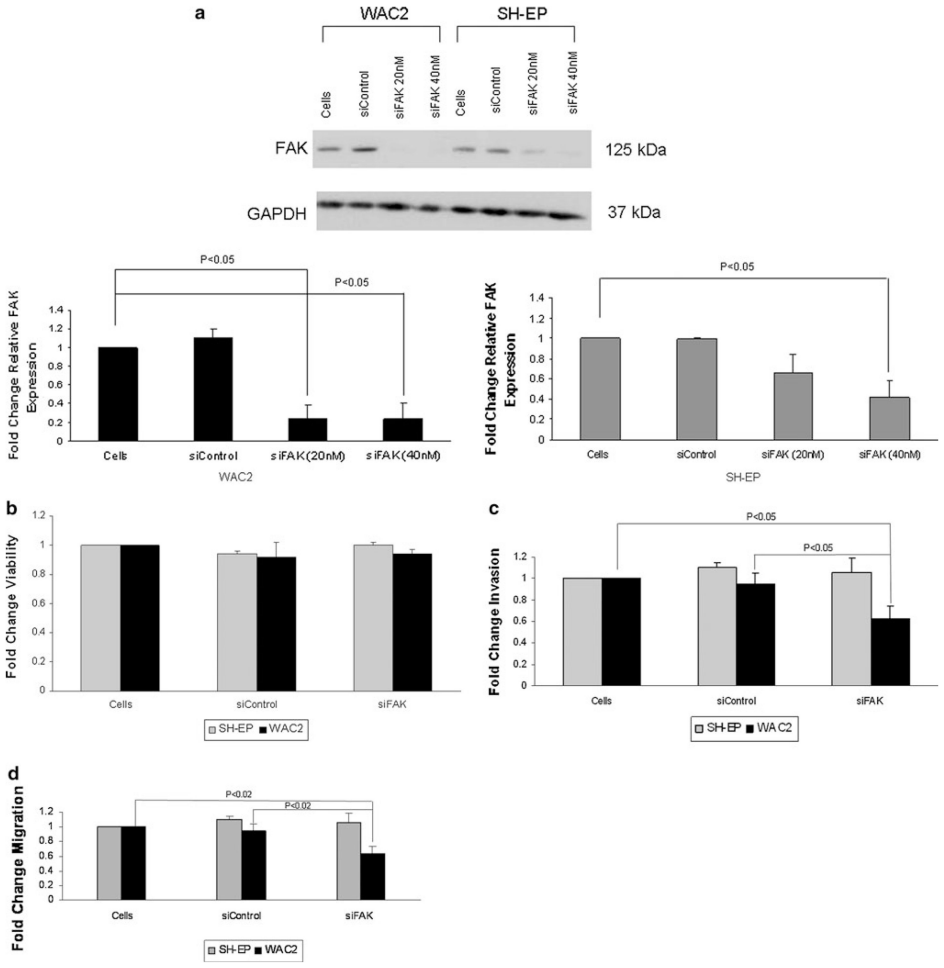

Fig. 2.

Focal adhesion kinase (FAK) inhibition with RNA silencing decreased invasion and migration in MYCN isogenic neuroblastoma cell lines. MYCN isogenic neuroblastoma cell lines, WAC2 (MYCN +) and SH-EP (MYCN−), were used to compare the effects of FAK inhibition in MYCN + versus MYCN− neuroblastoma cells. **a** WAC2 and SH-EP neuroblastoma cell lines were treated with FAK siRNA for 24 h. Immunoblotting was utilized to detect FAK protein knockdown. There was a significant decrease in FAK expression in both cell lines with 40 nM treatment siRNA, confirmed by densitometry (*bottom graphs*). FAK expression was not altered with the control siRNA. **b** The isogenic MYCN ∓ neuroblastoma cell lines, SH-EP and WAC2, were treated with siRNA knockdown of FAK (40 nM for 24 h). Cell viability was measured with alamarBlue® assays, and as seen with the non-isogenic MYCN cell lines SK-N-AS and SK-N-BE(2), there was no significant change in cell survival in either cell line with the siRNA FAK inhibition. Control siRNA did not alter cell survival in either cell line. **c** Cellular invasion was measured following FAK inhibition with siRNA (40nMfor 24 h) in the SH-EP and WAC2 cells. After 48 h, there was a significant decrease in the invasion of the MYCN + WAC2 cell line following FAK inhibition, but little change in invasion was seen with the MYCN- SH-EP cell line. These results were similar to those noted with the non-isogenic cell lines treated with FAK siRNA (Fig. 1c). Invasion was unaffected in either cell line with siControl. **d** The SH-EP and WAC2 cell lines were treated with FAK siRNA (40 nM for 24 h), and cellular migration was evaluated. Following 24 h, there was a significant decrease in

the migration of the WAC2 cells treated with FAK siRNA. There was nominal change in the migration of the SH-EP cells. Control siRNA treatment did no affect migration in either cell line

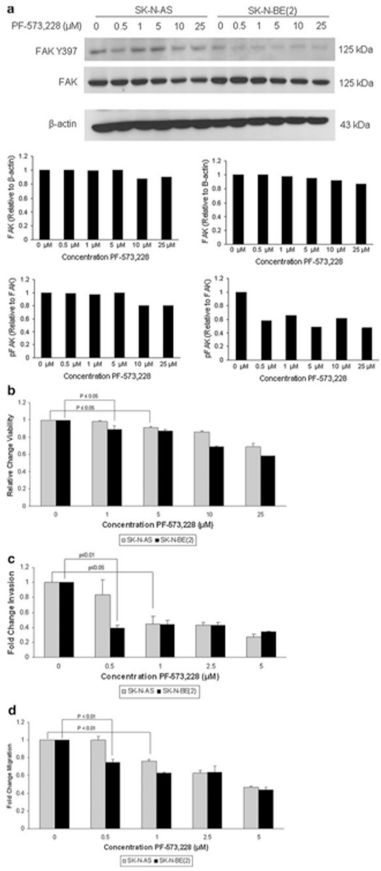

Fig. 3.

FAK inhibition with PF-573, 228 resulted in decreased neuroblastoma cell invasion and migration. **a** SK-N-AS and SK-N-BE(2) neuroblastoma cell lines were treated for 24 h with increasing concentrations of PF-573, 228. Immunoblotting was utilized to examine FAK Y397 phosphorylation and FAK expression. Densitometry was performed, and total FAK expression was reported as a ratio between the density of the FAK band to that of the band for β-actin. FAK phosphorylation was reported as a ratio between the density of the Y397 phospho-FAK band to the density of the total FAK band. In the SK-N-AS cell line, increasing concentrations of PF-573, 228 resulted in little change in FAK phosphorylation (*blot and bottom left graph*) but a small decrease in total FAK expression once high doses of PF-573, 228 were used (*blot and top left graph*). In the SK-N-BE(2) cell line, there was little change in total FAK in the SK-N-BE(2) cell line (*blot and top right graph*), but a significant decrease in FAK phosphorylation even with a small dose of PF-573, 228 (*blot and bottom right graph*). **b** AlamarBlue® assays were used to measure cell viability. SK-N-AS and SK-N-BE(2) neuroblastoma cell lines were treated with PF-573, 228 at increasing concentrations for 24 h. Cellular viability was significantly decreased in both cell lines following treatment, but the effects were seen at a lower concentration of PF-573, 228 in the *MYCN* amplified SK-N-BE(2) cell line. **c** SK-N-AS and SK-N-BE(2) cell lines were treated with increasing concentrations of PF-573, 228 and allowed to invade through a Matrigel™ coated micropore insert. Invasion was reported as fold change. Cellular invasion was significantly decreased in both cell lines with PF-573, 228 treatment, but a significant effect was seen at a lower concentration of PF-573, 228 in the SK-N-BE(2) cell line. Invasion was also decreased at concentrations less that those affecting viability. **d** SK-N-AS and SK-N-BE(2) cell lines were treated with increasing concentrations of PF-573, 228 and allowed to

migrate through a micropore insert. Migration was reported as fold change in number of cells migrating through the membrane. Cellular migration was significantly decreased in both cell lines with PF-573, 228 treatment, and as seen with invasion, the effects of PF-573, 228 upon migration were apparent at a lower concentration in the *MYCN* amplified SK-N-BE(2) cell line

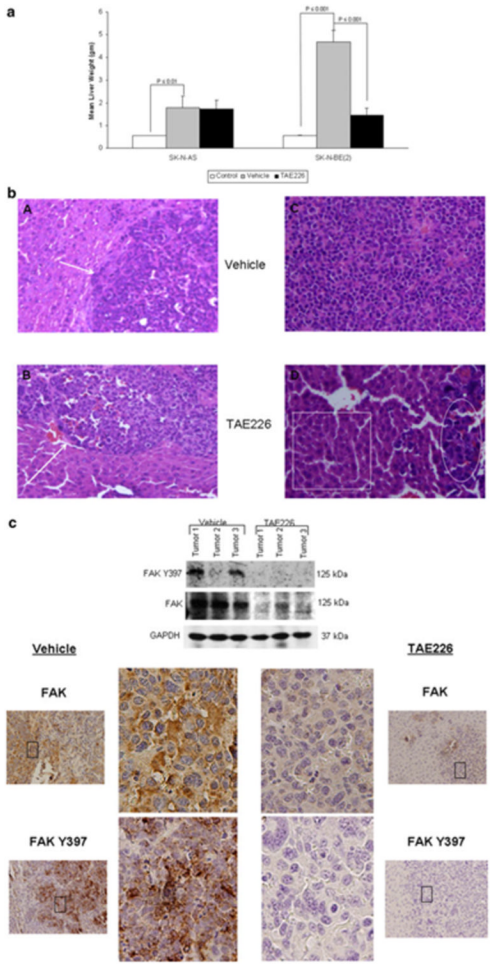

Fig. 4.

FAK inhibition resulted in decreased hepatic metastasis in a neuroblastoma nude mouse model. A nude mouse model was employed to study the in vivo effects of FAK inhibition on hepatic neuroblastoma metastasis. Neuroblastoma liver metastasis were induced by injecting either SK-N-AS or SK-N-BE(2) tumor cells into the sub-capsular space of the spleen. The mice ($N = 5$ per group) were treated with oral gavage of TAE226 or vehicle (*methylcellulose*) for 5 weeks. After 5 weeks, the animals were euthanized and the livers were harvested and weighed. **a** The weights of livers from non-injected control mice were included as a comparison (*white bars*). Liver metastasis formed in the mice injected with both SK-N-AS (1.78 ± 0.51 vs. 0.56 ± 0.035 gm, $p = 0.002$, cells vs. control, *grey* vs. *white bar*) and SK-N-BE(2) (4.67 ± 1.4 vs. 0.55 ± 0.042 gm, $p = 0.0006$, cells vs. control, *grey* vs. *white bar*) tumor cells. However, the SK-N-BE(2) mice developed a greater hepatic tumor load than the SK-N-AS injected mice [1.78 ± 0.5 vs. 4.67 ± 0.51 gm, $p = 0.0004$, SK-N-AS vs. SK-N-BE(2)]. In the SK-N-AS injected mice treated with TAE226 there was no significant decrease in the liver tumor burden (*grey* vs. *black bars*). In the SK-N-BE(2) injected mice, treatment with TAE226 significantly decreased the tumor burden in the liver (4.67 ± 0.51 vs. 1.46 ± 0.29 gm, $p < 0.001$, vehicle vs. TAE226) (*grey* vs. *black bars*). **b** Representative photomicrographs of hematoxylin and eosin (20×) staining of livers from animals injected with SK-N-AS and SK-N-BE(2) neuroblastoma cells. In the SK-N-AS animals treated with vehicle alone, there were more distinct deposits of tumor cells located all throughout the hepatic parenchyma (*panel A, white arrow*). TAE226 treatment of the SK-N-AS animals did not change the pattern of metastasis (*panel B, white arrow*), consistent

with the lack of changes in tumor burden (Fig. 4a). In the vehicle treated SK-N-BE(2) animals, there was diffuse infiltration of the liver parenchyma with small, round, blue tumor cells, and a loss of normal liver architecture (*panel **C***). After the SK-N-BE (2) animals were treated with TAE226, there were only scattered deposits of tumor cells (*panel D, white oval*) amongst normal appearing hepatocytes within normal hepatic architecture (*panel D, white box*). **c** Tumor specimens were homogenized and proteins separated on SDS-PAGE gels. Immunoblotting for FAK and FAK Y397 was performed. In the SK-N-BE(2) specimens, there were decreases in both FAK and FAK Y397 in tumors from animals treated with the FAK inhibitor, TAE226 versus those treated with vehicle alone (*top panel*). There were negligible differences in the SK-N-AS tumors (*data not shown*). Representative photomicrographs at 20× of immunohistochemical staining of the formalin-fixed, paraffin-embedded samples (*far left and far right panels*); larger images correspond to black box in photomicrographs. Immunohistochemical staining showed findings similar to immunoblotting; the tumors from the animals treated with TAE226 had decreased FAK expression and FAK Y397 phosphorylation (*right panels*) compared to the vehicle treated tumors (*left panels*)